

The microstructure of cement paste and concrete—a visual primer

Sidney Diamond *

School of Civil Engineering, Purdue University, West Lafayette, IN 47907-1284, USA

Abstract

This paper represents an attempt to provide an introduction to the microstructure of cement paste and concrete as seen in backscatter-mode scanning electron microscopy (SEM). Illustrations are provided of the ‘internal architecture’ underlying the microstructure of hardened cement paste and paste in concrete, at the size scales accessible to this instrument. Concrete is a uniquely complex engineering material. The aim of this paper is to provide researchers and practitioners who deal with it an acquaintance with its internal structure.

© 2004 Elsevier Ltd. All rights reserved.

Keywords: Microstructure; Scanning electron microscopy (SEM); Hardened cement paste (hcp); C–S–H gel; Pore structure

1. Introduction

As indicated in the title, this paper is an attempt to provide a ‘visual primer’ illustrating the important features of hydrated cement paste (hcp), both in separate preparations and in concrete, as seen in backscatter-mode scanning electron microscopy (SEM).

The approach employed is purely qualitative. The writer feels that solid qualitative understanding of the internal features of the material is essential before the implications of quantitative studies can be meaningfully addressed.

The coverage is confined to pastes and concretes made with ordinary Portland cement and excludes the special features associated with blended cements and with “high performance” concretes. It also excludes the specific microstructural features associated with carbonation, alkali silica reactions, sulfate attack, corrosion, freezing and thawing, delayed ettringite formation, etc., all of which may also be usefully examined by backscatter SEM.

The writer’s motivation in assembling this paper arises from his belief that the internal structures of hydrated cement pastes and concretes are poorly understood by most concrete engineers and technologists, and even by many researchers. The subject is inadequately treated in the few available textbooks on concrete, and often in the technical literature in general.

It should be realized that backscatter SEM is only one method of observation, and does not by itself provide a complete characterization of cement paste microstructure. It has various limitations. In addition to limitations on magnification, backscatter SEM observations are necessarily made on a two-dimensional surface, albeit one that is presumed to be representative of the structure. As indicated by Scrivener [1], details of the three-dimensional structure have to be inferred from the observations made on the two-dimensional surface. There is a further limitation in that only a small portion of the surface exposed in a given specimen is usually documented with micrographs. Selecting and imaging the areas to be documented generally involves some interpretation of what is present; such interpretations may vary among different investigators.

Despite these limitations, in the writer’s view, backscatter-mode SEM permits a clear assessment of the ‘internal architecture’ of hydrated cement systems, to an extent that is obtainable by no other means. In the present paper he has attempted to select representative images to provide a survey of the features of hcp that will be useful to non-specialist concrete researchers and engineers.

2. Details of backscatter-mode SEM examination

2.1. Instrumentation

Backscatter-mode SEM is one of a number of different SEM imaging techniques. All of them have the

* Tel.: +1-765-494-5016; fax: +1-765-496-1364.

E-mail address: diamond@ecn.purdue.edu (S. Diamond).

common feature of focusing a high-velocity electron beam on an extremely fine spot on the surface of a specimen, and then causing the focused beam to execute a raster pattern over the limited area of the specimen surface to be imaged. Various interactions of the electron beam occur with the atoms making up the rastered area, providing the possibility of a number of different modes of imaging.

In the early days of SEM, nearly all imaging of cement systems was done on specimens exposing fractured surfaces using a secondary electron detector. This method is still occasionally used. While individual features can be imaged at quite high magnifications, little information is forthcoming as to how the features fit together in terms of the internal architecture of the system.

In contrast, split-quadrant backscatter SEM detectors use flat polished specimens and provide images based on variations in electron backscatter coefficients of different areas. Differences in backscatter coefficients primarily reflect differences in chemical composition among the different features present. Chemical components of high electron density have high backscatter coefficients, and appear bright in the backscattered images. Conversely, components of lower electron density, such as most cement hydration products, have lower backscatter coefficients, and appear less bright.

The images are most useful if all topographic features are removed, i.e. if the specimen presents a flat, planar, and highly polished surface to the electron beam. To some extent the specimen preparation resembles the preparation of thin sections or polished surfaces ordinarily used in optical microscopy. However the physics of forming the SEM image is much different than the physics of forming optical images, and details that can be imaged in the SEM considerably exceed what is possible with even the finest optical instrumentation.

A brief discussion of how backscatter SEM detection systems function has been provided by Scrivener [1] in the present Journal issue. Those interested in more detail are referred to standard textbooks in the field, for example [2].

Additionally, and most important, nearly all backscatter SEM instruments are also equipped with energy-dispersive X-ray spectroscopy (EDX) systems, which can almost instantly provide specific chemical compositional information on any desired spot or area in the image being observed. This feature helps make backscatter SEM an extremely powerful and informative technique in concrete investigations.

2.2. Size scales in backscatter SEM examination

Since the sizes of images are often changed in printing, nearly all SEM instruments provide a scale bar as part of the image. A scale bar facilitates rapid exami-

nation of the sizes of the features being observed, and is a tool in properly assessing morphological details. Unfortunately, scale bars generated by the SEM instruments sometimes reproduce badly, and for clarity authors often provide a scale bar overlaid on the image itself. Both types of bar are used in the present paper.

Until recently, useful magnification in conventional backscatter SEM examination of cement systems almost never exceeded $4000\times$ even with the highest quality equipment. This permits rendering of details of sizes down to fraction of a μm , but nanoscale structural details are not accessible. Nevertheless many or most of the important features in hydrated cements are within the accessible range of magnification for backscatter-mode SEM. Indeed, most examinations of cement systems have been carried out at magnifications between $200\times$ and $2000\times$, with scale bars of $10\text{ }\mu\text{m}$ or larger being commonly shown in the image.

However, as illustrated by Kjellsen and Justnes in the present Journal issue [3], significantly higher resolution in backscatter-mode SEM can now be obtained using current generation *field-emission* SEMs (FE-SEMs); details finer than $0.1\text{ }\mu\text{m}$ are accordingly visible.

Backscatter-mode SEM provides a special advantage in that one may view the microstructure starting at a relatively high magnification appropriate to study the details of individual features, and then proceed to view the feature and the area surrounding it at progressively *lower* magnifications. This provides the ability to see how the individual features fit together in the total structure, an ability that is difficult or impossible with other modes of electron microscopy.

2.3. Specimen preparation

Specimen preparation for backscatter-mode SEM does not differ appreciably from preparation normally used for petrographic examination of concretes, except that a finer polish is essential, and a conductive coating needs to be applied to the final polished surface. A detailed description of all of the specific steps used in one laboratory has been published by Stutzman and Clifton [4], and another, more recently, by Kjellsen et al. [5]. There are many minor variations on these basic procedures used by different laboratories, but comparison of published micrographs from different laboratories suggest that these variations are in fact unimportant. It has long been considered that drying in specimen preparation may alter the nanoscale structure of C–S–H, but such alteration, if it occurs, is not detectable in backscatter mode SEM. A very occasional shrinkage-induced microcrack may be observed, but it is never certain whether a given microcrack was induced in the specimen preparation or was present in the original paste or concrete. One major artifact commonly observed is the characteristic shrinkage of ettringite masses on dehy-

dration, which produces a so-called “tiger stripe” morphology such seen in Fig. 7; this artifact is actually extremely helpful in spotting ettringite when it occurs in masses rather than in isolated crystals.

2.4. Digital imaging

In recent years almost all microstructural imaging of cement paste and concrete has been recorded digitally instead of on the photographic film previously used. A few years ago the writer provided a discussion of the pros and cons of digital imaging and reproduction, especially for hydrated cement systems [6]. The advantages of acquiring, storing, manipulating, and publishing micrographs in digital form are now generally appreciated.

3. The microstructure of hydrated cement paste

3.1. Introduction

The microstructure of hydrated Portland cement pastes varies considerably with such factors as the chemistry and fineness of the cement used, the water: cement ratio, the use of chemical admixtures, variations in mixing procedures, differences in early curing temperatures, and variations in hydration conditions. Nevertheless, most cement pastes show common features, and descriptions of these as they appear in backscatter mode SEM are attempted here.

It should be pointed out that the use of backscatter SEM for examinations of cement pastes and concretes was pioneered by Scrivener and Pratt [7], not so many years ago. Unfortunately, further investigations have been pursued only in relatively few laboratories around the world, although SEMs are commonly available in universities and research institutes.

The utility of EDX instrumentation in conjunction with backscatter SEMs has already been mentioned; specific chemical information is often essential to check the interpretations being made while conducting an investigation.

3.2. Residual Portland cement grains and surrounding hydration shells

Unhydrated remnants of Portland cement particles are retained in all or nearly all cement pastes, and are readily identified as such. The clinker components (C_3S , C_2S , C_3A , ‘ C_4AF ’ and several minor components) are all crystalline, with typical crystal sizes ranging from about 1 μm to as much as 60 μm . Clinkers are normally ground to sizes between about 2 μm to about 80 μm ; the typical mean diameter is usually of the order of 10–12 μm . In general, the grinding does not separate individual

crystals, but breaks up the clinker mass as a whole. Thus most individual grains in cement contain fragments of several different kinds of crystals which were adjacent to one another in the clinker; the larger grains may contain some unbroken crystals as well. Small intact crystals of the interstitial components (C_3A and ‘ C_4AF ’) are almost always present in the larger cement grains.

Quantitative and qualitative features of Portland cement clinkers as they appear in backscatter SEM have been illustrated by Stutzman [8] in the present Journal issue.

When cement hydrates, the innermost parts of larger ground cement grains almost always remain in an unhydrated condition for a long time. Since the non-hydrated components in cement have much higher electron backscatter coefficients than the hydrated products, these residual unhydrated cement grains appear in backscatter SEM images as bright entities in a sea of darker areas.

Fig. 1 provides an illustration of this feature (and others) as seen in a w:c 0.30 paste examined after 100 days of room-temperature hydration.

Fig. 1 was taken at a relatively low magnification (approximately 500 \times). It displays an area about 180 μm in height and 230 μm in width, or about 41,000 μm^2 . This is a large enough area to include features representing a number of the original cement grains, and of course the originally water-filled spaces between them. The bright white areas of different sizes, more than a dozen of which are present, are unhydrated cores of individual cement grains, the largest being more than 40 μm in size, the smallest less than 5 μm . Most of these cement remnants are surrounded by, and are in close contact with, smooth-textured uniformly gray hydration product shells of varying thickness. A hydration shell that represents fully complete hydration is marked in the figure. These “inner product” hydration shells appear non-porous at this magnification. A few fully hydrated particles lacking the bright core of unhydrated cement can also be seen; one is so labeled. The original size of a given cement grain can readily be estimated as the sum of the sizes of the unhydrated core and the surrounding hydration shell. Most of the fully hydrated grains are slightly smaller than the grains with unhydrated cement cores. Actually there is no guarantee that a grain that appears fully hydrated on the plane of observation is in fact completely hydrated; there may be a residual unhydrated core existing above or below the plane being imaged.

These hydration shells (with their cement cores in most cases) are separated from each other by a groundmass of finer hydrated components of much less homogeneous appearance.

In backscatter SEM images the available range of black to white is customarily divided into 256 ‘gray levels’ or shades of darkness. The lowest level, usually recorded as gray level 0, is fully black; the highest level,

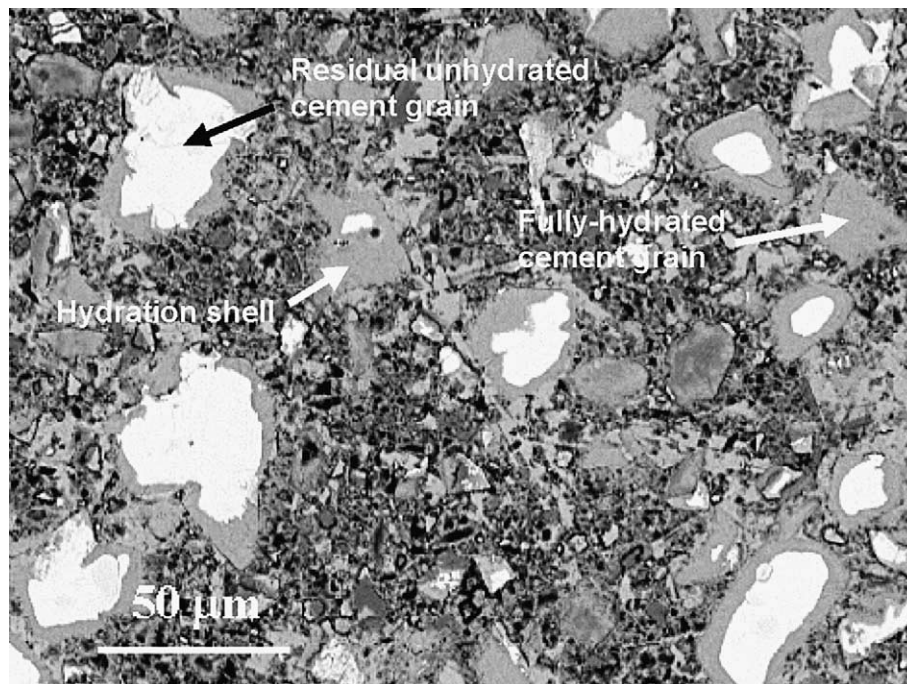


Fig. 1. View of the microstructure of a 100-day old w/c 0.30 cement paste, cured at room temperature.

usually recorded as gray level 255, is fully white. One speaks of darker areas on the image as areas of lower gray levels, and conversely of the brighter areas as areas of higher gray levels. In Fig. 1 it is obvious that the unhydrated remnants of the cement grains exhibit much higher gray levels than the hydrated components surrounding them.

In more nearly mature cement pastes (and concretes) the relative proportion of unhydrated cores is commonly smaller than that seen in Fig. 1. Nevertheless, a few such residual unhydrated cores are almost always present, unless the concrete has been subjected to extensive leaching over a long period. Furthermore, as will be illustrated later, small, bright ‘shards’ of unreacted C_4AF usually persist, even in cement pastes and concretes that are otherwise fully hydrated.

The hydration products found in most hardened Portland cement pastes or concretes primarily consist of C–S–H gel and calcium hydroxide, accompanied by smaller amounts of ettringite and monosulfate. These hydration products are intermingled with pore spaces. In the specimens as normally prepared, the pore spaces are not actually empty spaces but are occupied by hardened epoxy resin.

In the following sections an attempt is made to provide characteristic illustrations of each of these features of cement pastes.

3.3. C–S–H gel

C–S–H gel (sometimes shortened to simply ‘C–S–H’) is not a single substance, but rather constitutes a con-

venient collective term for a range of quasi-amorphous particles (and masses) containing calcium, silica, and water that have been produced by hydration of the C_3S and C_2S in cement. These products are deposited within the hardened cement paste structure by several different processes. The chemical composition is not quite constant in a given paste but may vary slightly from place to place, as does the internal porosity. As a result, the gray level for C–S–H is not entirely consistent, but shows some local variation.

Standard treatments of C–S–H gel, for example that of Taylor [9], consider it to be made up of two varieties: the so-called ‘inner product’ C–S–H, developed as hydration shells within the original boundaries of the cement grains, and the ‘outer product’ C–S–H, formed by through-solution deposition in the originally water-filled space. Some time ago, Diamond and Bonen [10] suggested an alternate nomenclature in which the individual identifiable grains of remnant cement cores *and* their surrounding hydration shells were described as ‘phenograins’, with the C–S–H of the hydration shell portion called ‘phenograin C–S–H’. The term phenograin is used in mineralogical nomenclature to connote distinct grains embedded in a groundmass of fine material. In this proposed nomenclature the finer textured and more porous C–S–H deposited in originally water-filled spaces between cement particles was termed ‘groundmass C–S–H’. This proposal has not been generally accepted.

The hydration shells pointed out in Fig. 1 are clearly ‘inner product’ or ‘phenograin’ C–S–H. As indicated previously, these hydration shells are smooth-textured

(at normal backscatter SEM magnification), and their gray level is mostly uniform.

This is not always the case. So-called ‘two-tone’ inner product hydration shells are known to occur in some cement pastes and concretes. In such two-tone inner products the slightly brighter layer is almost inevitably outside of the slightly darker layer, i.e. it represents the C–S–H that was formed earlier in the hydration sequence. The difference in gray level may represent differences in internal porosity (the brighter zone being less porous) or it may under certain circumstances reflect differences in composition. The subject is still being debated among investigators.

In contrast to the generally featureless texture of the hydration shells, the groundmass or ‘outer product’ deposited in the originally water-filled space is irregularly textured. A significant portion of Fig. 1 represents areas of such originally filled space. These areas appear mostly darker overall than the inner product hydration shells. They contain many individually recognizable pores, and a populations of finer pores too small to be resolved. In addition to the outer product C–S–H precipitated from solution, they also host extensive deposits of calcium hydroxide (CH) and the minor hydration products (ettringite, monosulfate, etc.).

It is an interesting point that not all individual cement grains generate hydration shells of appreciable thickness. Examples of some that do not are seen in Fig. 2,

taken from another area of the paste that was depicted in Fig. 1, at somewhat higher magnification.

Three specific grains are marked in Fig. 2. The grain marked “A” is a residual cement grain with a hydration rim of inner product C–S–H, as discussed previously. The grain marked “B” is quite different; here there is almost no evident inner product hydration shell. The grain marked “C” is fully hydrated, with no visible cement core.

Grain “B” is composed primarily of β -C₂S, and despite its lack of a significant hydration shell, it has in fact hydrated to some degree. The cross-hatched appearance it displays is characteristic of partially hydrated β -C₂S, a significant component of Portland cement. It appears that, unusually, almost the entire ground clinker grain was composed of β -C₂S. Other grains, not necessarily composed of β -C₂S, may also show little surrounding inner product. An example is the complex white grain below and slightly to the right of the fully hydrated grain marked “C”.

The tendency to form hydration shells around individual cement grains is thus not universal. The relative proportions of grains that do not do so may vary from place to place in a given specimen. It may also vary with different cements [11].

Most of the areas depicted in Fig. 2 are groundmass areas not associated with any specific cement grain; rather they reflect fine-textured outer product C–S–H and

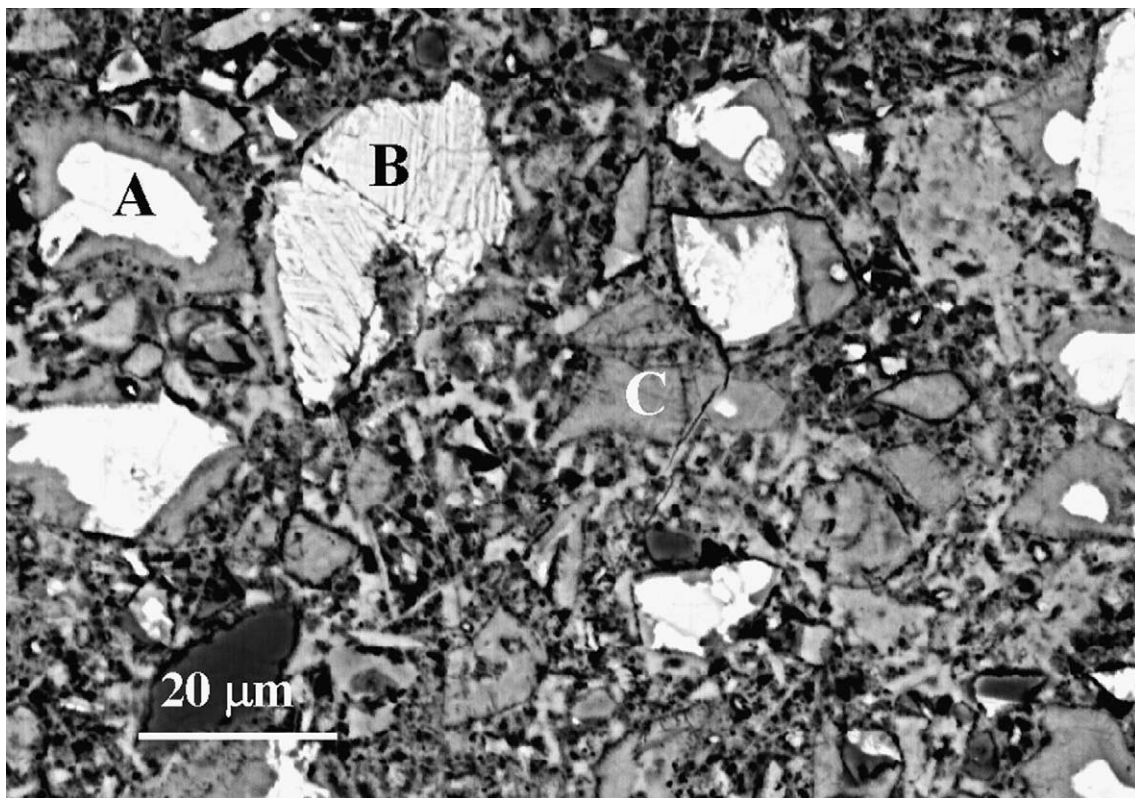


Fig. 2. An area in the 100-day old w/c 0.30 paste at higher magnification.

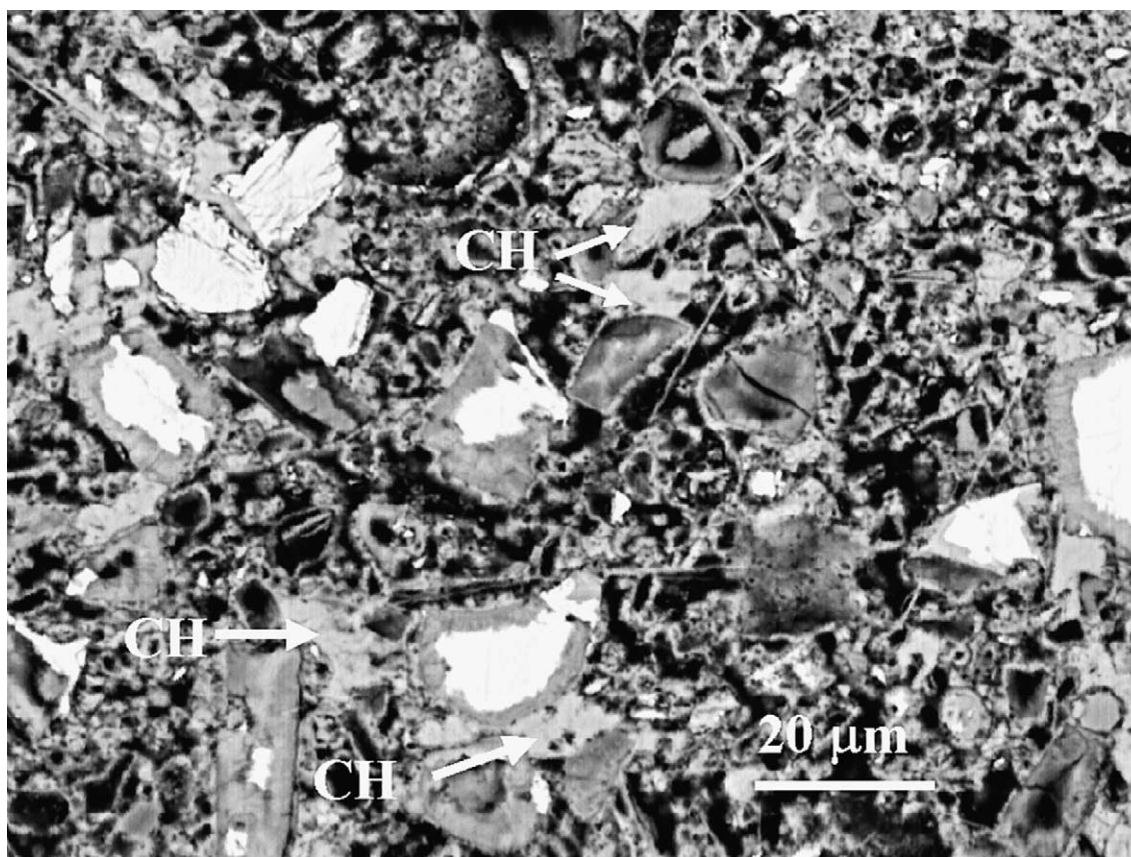


Fig. 3. An area from a 7-day old w:c 0.45 cement paste, showing details of the porous groundmass and CH deposits.

other components deposited in originally water-filled space.

Figs. 1 and 2 are taken from a fairly dense mature paste of low water:cement ratio (w:c 0.3). In contrast, Fig. 3 shows the structure of a younger and substantially less dense paste, this one a 7-day old room-temperature hydrated paste prepared at 0.45 water:cement ratio. The magnification is the same as that of Fig. 2, to which it may be compared.

The ‘phenograins’ representing the larger reacted or partly reacted cement grains in Fig. 3 are more or less similar to those of Fig. 2, but the groundmass areas between them are quite different. Much of the groundmass seen in Fig. 3 is made up of distinctly visible black pores, many in the multi-micrometer size range. A substantial proportion of the pores are surrounded by thin-walled brighter shells, some of which are linked together. The shells are one variety of outer product C–S–H.

Less prominently featured in Fig. 3, but of considerable importance are a number of irregular deposits of somewhat brighter appearance than the C–S–H. These are calcium hydroxide (CH); four of them are marked as such in the figure, and there are several others. In this paste their size range is of the order of 10–15 μm.

Further details of the cellular structure found in the groundmass of young cement pastes are seen in Fig. 4, taken at higher magnification. The paste here is a 1 day old w:c 0.45 paste hydrated at room temperature. A typical thin walled cell about 5 μm in size is marked “A” in the figure. The hollow cells are of various shapes, from the triangular one marked “A”, to almost rectangular, to oval; some are elongated. While the thin-walled cell structures predominate in the groundmass, there are various nondescript particles of similar gray level that are not cellular, such as the one marked “B” in the figure. Both types of particles have C–S–H compositions, and both have been previously recognized and described by Diamond and Bonen [10].

Fig. 4 also contains several larger features, one of which is marked “C” in the figure. This feature is obviously a residual cement grain, but it does not show a close-fitting hydration shell. Rather a thin shell is present, surrounding, but separated from the residual core leaving a distinct (but partial) gap. Such gaps are visible around the other residual cement grains depicted in the figure. The thicknesses of most of the shells are less than one μm, similar to those of the groundmass cellular structures discussed earlier.

Partially or fully hollow-shell grains were first observed by Hadley many years ago [12], using secondary

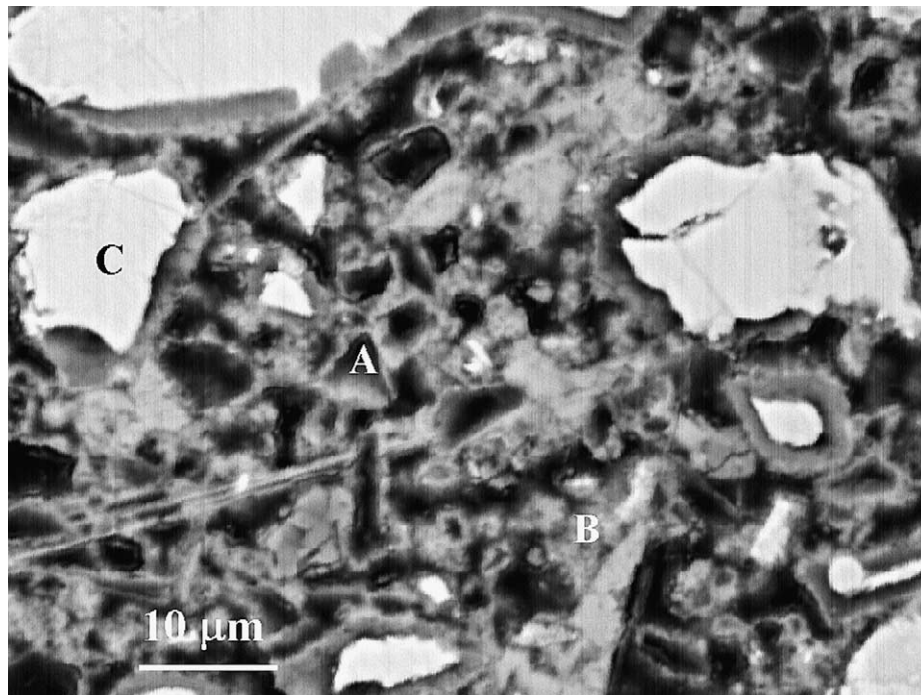


Fig. 4. Area in a 1 day-old w:c 0.45 paste showing cellular structures and the hollow-shell hydration mode.

electron mode SEM. Hadley observed that, instead of producing a hydration shell maintaining close contact with the residual core, some cement grains deposit only a thin shell of C–S–H and then ‘hollow out’ internally, partly or completely. An annotated extract of relevant portions of Hadley’s thesis was recently published [13].

The cellular structures of the groundmass in Figs. 3 and 4 almost certainly represent fully hollowed out shells formed within the first day’s hydration from the finest particles of the ground cement. Larger cement grains hollow out more slowly, and many of them subsequently fill in with freshly precipitated C–S–H.

Despite the reluctance of some authorities to accept the hollowing out process as a normal component of cement hydration, these so-called “hollow shell grains” or “Hadley grains” in various sizes are readily visible in many cement pastes, and have been documented by many authors.

The microstructure shown in Fig. 4 represents the internal architecture of a young, incompletely hydrated paste; it should not be taken as a representation of the final state of hcp microstructure. As hydration proceeds, the open cellular groundmass seen in Fig. 4 is progressively filled in with new hydration products, and its texture becomes progressively more dense. Thus the open cellular structures are not generally detected in mature pastes or concretes, especially those of low water:cement ratios. Furthermore, the visual distinction between inner and outer product C–S–H (or pheno-grains and groundmass) becomes increasingly more

difficult to make, as the hydration products tend to fuse into a nearly continuous mass.

Such a condition is shown in Fig. 5, which displays an area within a w:c ratio 0.45 concrete that has been allowed to hydrate under water for several years at room temperature, and is virtually completely hydrated. The figure contains two images. The image to the left (to which the upper 100-μm scale bar applies) was taken at a lower magnification; originally 250×, and it shows a large area of dense hardened cement paste (hcp). The image to the right, to which the lower 10-μm scale bar applies, represents the area within the outlined box, and was taken to show more detail. The large elongated uniform gray grain in the center of the left image is a sand grain; the narrow and relatively bright deposit below it is a layer of calcium hydroxide (CH). In the right image a number of bright shard-like grains can be distinguished within the dense hcp; these are remnants of unhydrated C₄AF. A few pores of appreciable size remain in the mostly dense mass; these are residual hollow shell pores that were never filled in with late hydration products.

3.4. Calcium hydroxide

Calcium hydroxide is an important product of cement hydration. As previously indicated, it can be distinguished in cement pastes by a gray level slightly brighter than that of C–S–H gel, although the distinction sometimes requires close examination. Despite its

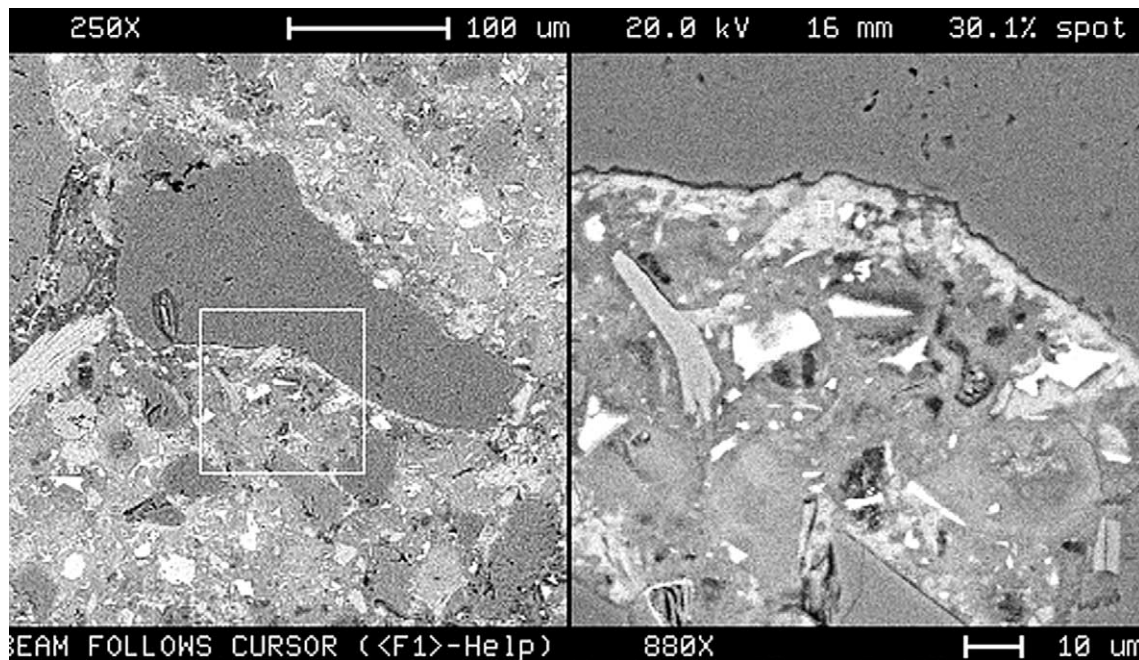


Fig. 5. Dense internal structure in a virtually completely hydrated w:c 0.45 concrete.

well-documented internal crystallinity, CH within cement pastes usually appears as irregular masses of various sizes, rather than as euhedral crystals. Small patches of CH in cement paste were pointed out in Fig. 3, and a layer of CH bordering the sand grain was pointed out in Fig. 5. Somewhat larger and much more irregular CH

deposits appear in Fig. 6, taken from a 7-day old w:c 0.45 room temperature hydrated cement paste.

The present writer recently compiled the results of a number of earlier studies detailing the morphology and distribution of sizes of CH in various cement pastes and concretes [14].

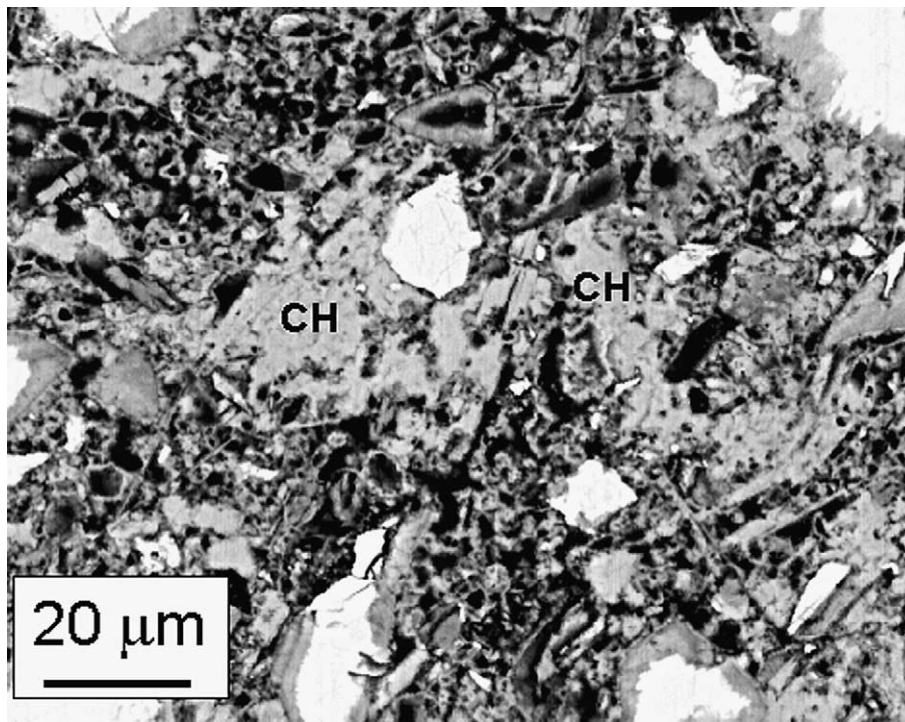


Fig. 6. Irregular calcium hydroxide deposits in a 7-day old w:c 0.45 paste.

3.5. Minor components

Two forms of calcium aluminate sulfate hydrates, ettringite and monosulfate, are usually found in small quantities in most cement pastes. Both can sometimes be seen in isolated deposits or pockets within the originally water-filled space; more usually, they are intimately intermingled with outer product C–S–H and CH in the groundmass, and are difficult to recognize. Much larger masses of ettringite can be found as secondary products in sulfate attack, often in air voids. Ettringite is also found in cracks and rims surrounding aggregates in concretes subject to delayed ettringite formation (DEF).

Ettringite in masses usually displays a characteristic shrinkage-induced pattern of curved cracks, which has been described as “tiger stripe” morphology. An example of such a mass is shown in Fig. 7, filling an air void in a concrete. Much smaller pockets of ettringite are also present in the surrounding hcp, but they are difficult to detect. The EDX spectrum shown to the right of the image in Fig. 7 is characteristic for ettringite, and was taken from a spot near the center of the mass.

Unlike ettringite, monosulfate masses tend to show straight ‘cleavage-like’ shrinkage features. Two examples, found in pockets within the paste of a mature fly-ash bearing field concrete are marked by arrows in Fig. 8. The EDX spectrum taken from the monosulfate deposit in the center of the image, is provided at the right of Fig. 8. The spectrum is quite characteristic for monosulfate. In contrast to the spectrum for ettringite in Fig. 7, for monosulfate the peak for sulfur is characteristically smaller than the peak for aluminum.

The distinction between the ‘tiger stripe’ and the ‘cleavage’ shrinkage-induced morphologies is usually apparent, but the proper identification of any deposit whose morphology may not be clear can readily be accomplished by EDX.

3.6. Pore space

Significant contents of visible pore space can usually be detected by backscatter SEM in most cement pastes. The actual content depends mostly on w:c ratio and degree of hydration. The preceding figures show clear indications of such pores. The low electron backscattering ability of the epoxy resin that fills the pore space in prepared specimens causes such areas to appear much darker than even the hydrated cement constituents.

Image analysis can be used to quantify the content of detectable pore space in a given paste. As shown in the paper by Sahu et al. [15] in the present Journal issue, such analysis can provide a reliable estimate of the water:cement ratio in well hydrated cement pastes or concretes.

The sizes of pores that can be detected in backscatter SEM is limited by the resolution of the images; to be recognizable as such, the pores must a number of contiguous dark pixels. At the usual range of magnifications, this generally means that pores of sizes less than about 0.2 μm are not easily resolved. However, as indicated in the paper by Kjellsen and Justnes [3] much finer pores can be seen in FE-SEM examination. Nevertheless, the *lower limit* of conventional SEM-detectable pore sizes is usually larger than the *upper limit* of

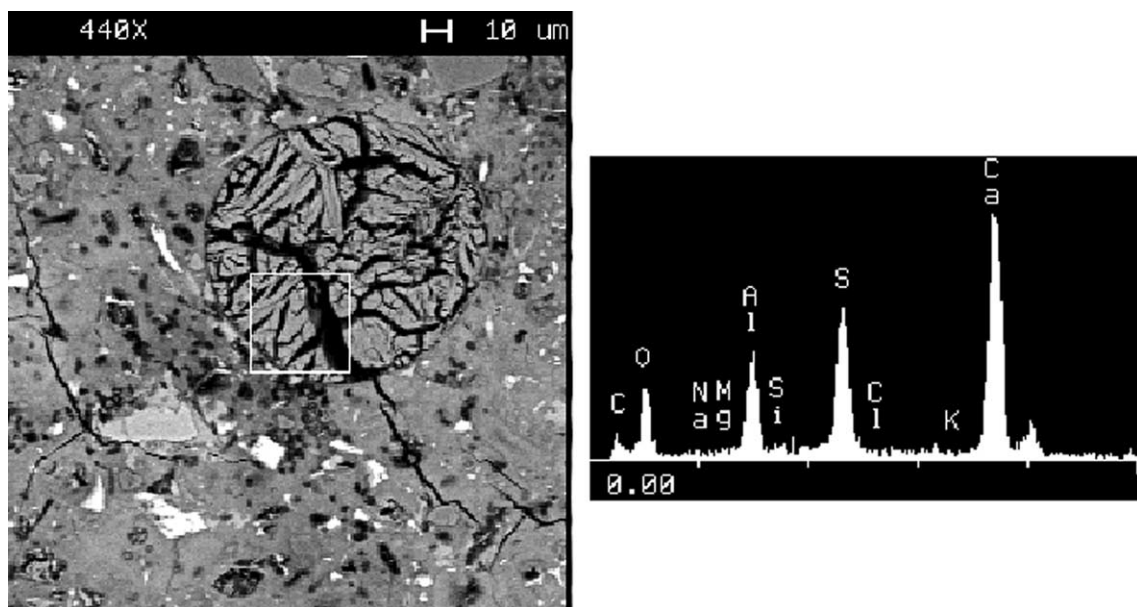


Fig. 7. An ettringite mass deposited in an air void in a field concrete, showing the characteristic “tiger stripe” morphology. The EDX spectrum is characteristic for ettringite.

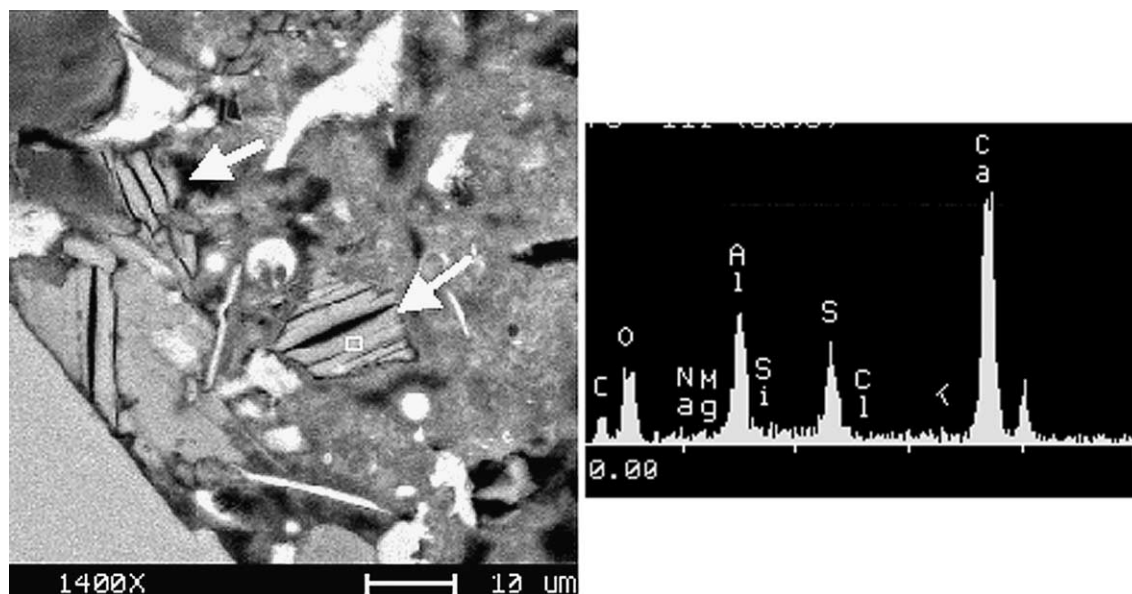


Fig. 8. Appearance of monosulfate deposited within paste pockets in a mature, fly-ash bearing field concrete.

pore sizes reported in mercury intrusion porosimetry studies of hydrated cement paste [16]; the latter is often significantly less than 0.1 μm. Thus SEM examinations quite conclusively show that the commonly-used mercury intrusion method vastly underestimates the sizes of the pores that are actually present in a given paste. Despite its common acceptance, mercury intrusion is not of value in determining actual pore size distributions in hardened cement pastes and concretes.

In SEM examination, most cement pastes reveal the presence of several different kinds of pores. Occasional spherical air voids, which are usually much larger than any other type of pore present in cement systems, are commonly found even if no air-entraining agent has been used. Pores arising from hollow shell hydration have already been illustrated. In pastes of reasonably high w:c, irregular pores can usually be detected that appear to be residues of the originally water-filled space, thus fitting the classical definition of capillary pores. Such pores are convoluted in outline, and often appear interconnected. In contrast, the hollow shell pores are less convoluted in shape and are surrounded by recognizable thin shells. Isolated residual hollow-shell pores are usually seen even in older, low w:c pastes where the C–S–H has fused into a massive deposit, and detectable “capillary pores” are no longer visible.

4. The microstructure of concrete

The characteristics of hcp within concrete are often little different from those of cement pastes by themselves. For example, Fig. 9, from a porous area in a briefly mixed 3-day old w:c 0.45 laboratory concrete

hydrated at room temperature, shows much the same paste microstructural features as those previously displayed for young cement pastes. These include unhydrated cement remnants (A), inner product C–S–H (B), calcium hydroxide (C), and a large area of porous groundmass containing many Hadley grains, both fully hollow fine grain shells (D) and partly hollowed out larger grains (E).

Concretes, however contain features not found in pastes, as discussed below.

4.1. Aggregates

Obviously, concretes contain both coarse and fine aggregates, components that are not found in cement pastes. Backscatter-mode SEM is not usually employed in studying or describing these components except in special cases, such as for example examinations of alkali-reactive aggregates.

Nevertheless, at low magnification backscatter-mode SEM examination can be useful. Such examination can readily distinguish between manufactured sand and rounded fluvial sand. It can provide information on the sizes and shapes of sand grains, and also of coarse aggregate grains, if the examination is conducted at a low enough magnification. Such examination can provide a qualitative indication of the spacing between aggregate grains, and an assessment of the volume percentage of paste in a given concrete can be made.

Nevertheless, most examinations of sand or aggregate in concrete are still carried out using optical microscopy rather than SEM; optical examination has the advantage that color distinctions can be made, and that the relevant optical properties of the minerals present can be

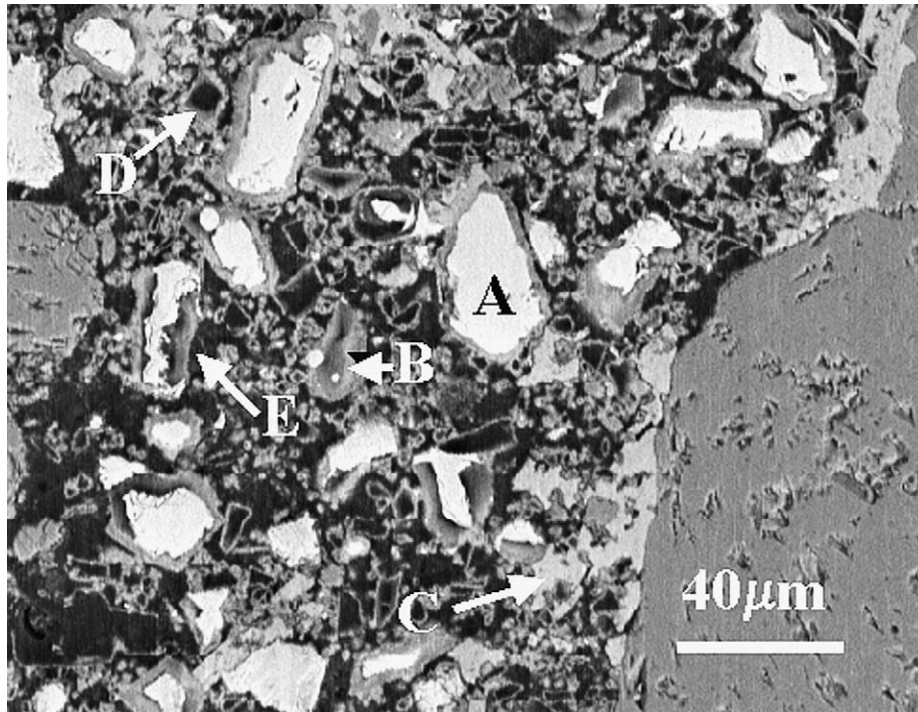


Fig. 9. An area in a 3-day old w/c 0.45 concrete; the microstructural features displayed are similar to those shown for hydrated cement pastes prepared without aggregates.

determined. On the other hand, backscatter-mode SEM with EDX has a major advantage in that the chemical compositions can be readily assessed.

4.2. Air voids

Many or most concretes are deliberately air entrained. In such concretes, air voids tend to occupy a high proportion of the non-aggregate space: values around 15% are typical. The size range found is mostly from about 20 μm to about 1 mm: thus air voids are much larger than most hcp features. A very low magnification backscatter-mode SEM view showing the appearance of air voids of typical size in a deliberately air-entrained paste is provided as Fig. 10.

Essentially all entrained air voids are spherical, leading to easy recognition in backscatter SEM. The relative content, spatial distribution, size distribution, and degree of separation between adjacent air voids all may be studied readily at low magnification. Since the plane of examination does not usually cut through the center of the spheres, the true air void diameters are somewhat larger than they appear in the SEM image.

Air voids generally show a thin lining of calcium hydroxide. In concretes exposed to wet conditions (or to alternate wetting and drying) air voids frequently show internal deposits of calcium hydroxide or ettringite or both. Such deposits are usually sparse, but in extreme cases they may entirely fill the air void. Such a case was illustrated of an ettringite deposit in Fig. 7.

4.3. Areas of cement paste adjacent to aggregates

Areas of cement paste adjacent to sand or coarse aggregate grains have been accorded a special status in the literature, as so-called “interfacial transition zones” (ITZs). Such zones have often been claimed to be regions of significantly higher porosity than the bulk of the cement paste. The innermost parts of such zones, i.e. those within only one or two μm from the aggregate, have been considered to be especially porous, an average detectable porosity of about 30% has been recorded [17].

In the writer’s experience there appears to be higher contents of detectable pores only within *some* (not all) local areas of hcp adjacent to aggregate surfaces, and the overall average of the incremental pore space detected seems to be small. Partly this is because a significant part of the aggregate surface is covered with a layer of CH that exhibits limited (or zero) porosity. Such CH deposits have appeared in Figs. 5 and 9 of the present paper. In the concretes the writer has examined, rough measurements suggested that about one-third of the aggregate surface exposed on the plane of observation is bounded by CH deposits of appreciable thickness, i.e. over 5 μm wide on the exposed plane.

Even where such CH deposits are locally absent, in many areas the paste adjacent to the aggregate appears to be of porosity similar to that shown by nearby ‘bulk’ hcp.

The extensive local porosity thought to be characteristic of the ITZ is usually considered to arise from the

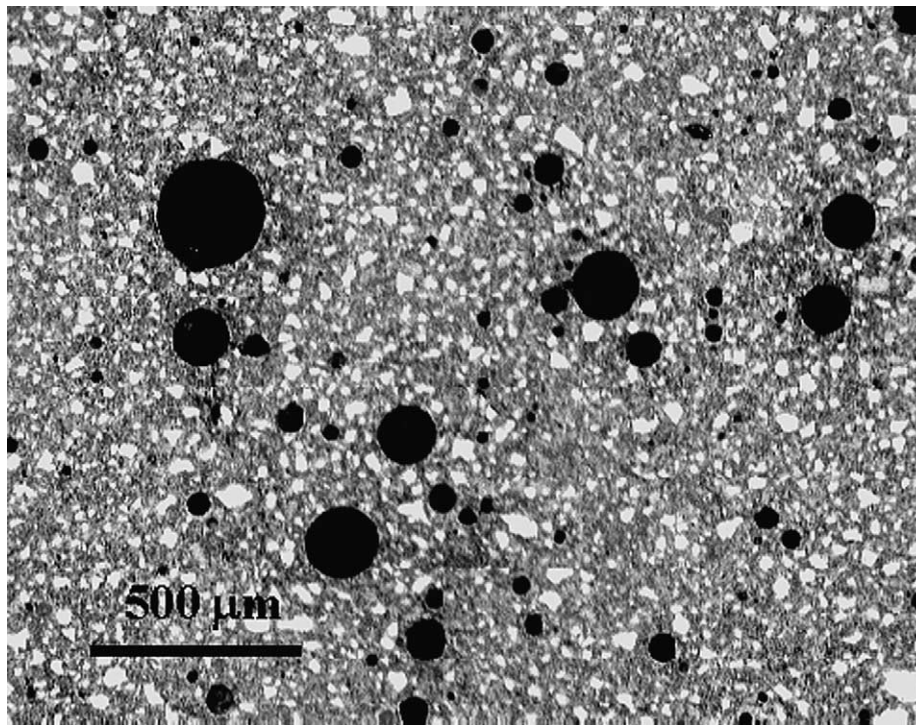


Fig. 10. Very low magnification view showing typical air void sizes in a deliberately air-entrained hardened cement paste.

local deficiency of cement particles close to the aggregate in the fresh concrete after mixing. This deficiency necessarily leads to larger proportions of water-filled space close to the aggregate surfaces *at the start of hydration*. However, it appears that much of the extra water-filled space adjacent to the aggregate is quickly occupied by calcium hydroxide deposits, or by C–S–H precipitated by the through-solution mechanism from more distant cement grains.

These observations have been checked with a number of normal concretes, and in the writer's experience they appear to be well-founded. The existence of the dense layer deposits of CH around much of the aggregate surface in normal concrete was very clearly described and documented by Bache et al. about 40 years ago [18].

Fig. 11 shows a representative area of paste adjacent to the surface of a crushed coarse aggregate grain in a 3-day old, thoroughly mixed w:c 0.5 laboratory concrete hydrated at room temperature. A dense, essentially non-porous layer of CH occupies the upper two-thirds of the aggregate-paste interface displayed. Where it occurs, this essentially non-porous layer occupies what would be considered the most porous part of the ITZ. The lower third of the aggregate-paste interface displayed in the figure lacks this CH layer, but shows no indication of excessive porosity next to the aggregate surface.

The relative sparseness of larger remnant cement grains in hcp adjacent to the aggregate can be seen in the figure. Nevertheless, some cement particles have approached, or in some cases have come close to the

aggregate surface. Such an “almost contact” of a large residual cement grain is visible in the lower left corner of the figure, and several smaller grains are even closer.

Fig. 12, from the same 3-day old w:c 0.5 concrete as Fig. 11, shows an interesting area. A roughly 50 μm-wide strip of hydrated cement is shown occupying the space between two aggregate grains. By convention, all of the strip would be considered as being within the two overlapping ITZs; and such space would conventionally be considered to exhibit a ‘percolated’ pore system.

There seems to be a transverse break across the paste strip, perhaps due to specimen preparation. Other than this, the microstructure displayed between the two adjacent aggregates reveals no unusual porosity, and appears to be representative of normal cement paste in a reasonably young w:c 0.5 concrete. Several relatively large residual cement grains are present, and a layer of calcium hydroxide is deposited over part of the surface of the lower grain. Some large hollow-shell pores are evident, but there is no indication of especially porous microstructure close to either of the aggregate surfaces; nor is there any indication of excessive pore space ‘percolating’ due to overlap of the ITZs from adjacent aggregates, as would be expected from conventional ITZ concepts.

It should be noted that the writer's experience and conclusions concerning the general existence of the ITZ in concrete is controversial; indeed a diametrically opposed point of view is expressed by Scrivener [1] in the present Journal issue.

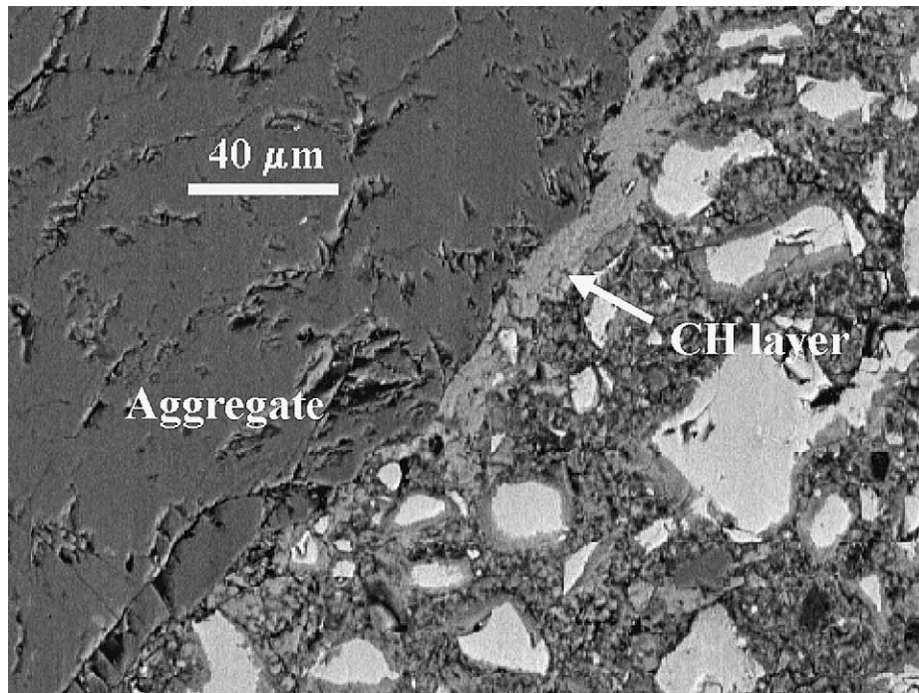


Fig. 11. View of a portion the zone of contact between aggregate and paste in a 3-day old w:c 0.5 concrete. A deposit of essentially non-porous CH covers most of the actual interface; the hcp zone below the CH layer does not show indications of excessive porosity, even immediately adjacent to the aggregate.

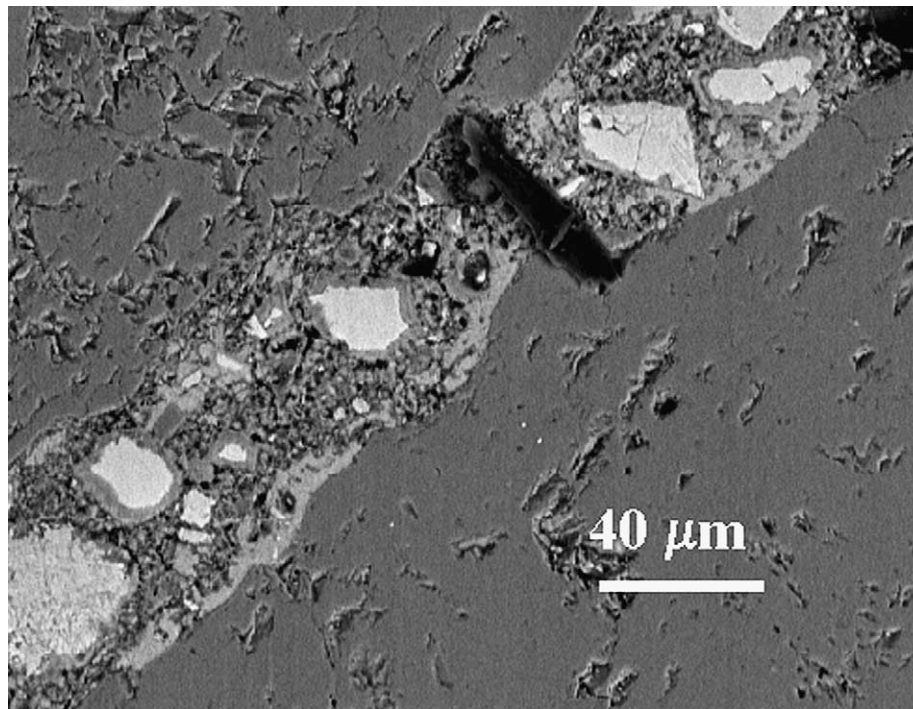


Fig. 12. Area of hcp between two closely spaced aggregate grains in a w:c 0.5 concrete. The paste shows normal microstructural features. There is no indication of excessive pore space 'percolating' due to overlap of ITZs from adjacent aggregates, as would be expected from conventional ITZ concepts.

4.4. Paste inhomogeneity in concrete—the “patch” effect

Nothing has been said previously about the homogeneity of cement paste in concrete on a broad scale, i.e.

when examined at magnifications lower than one ordinarily uses to study the details of individual features. In point of fact, cement paste in concrete of normal w:c ratios often appears as a “patchy” material at low

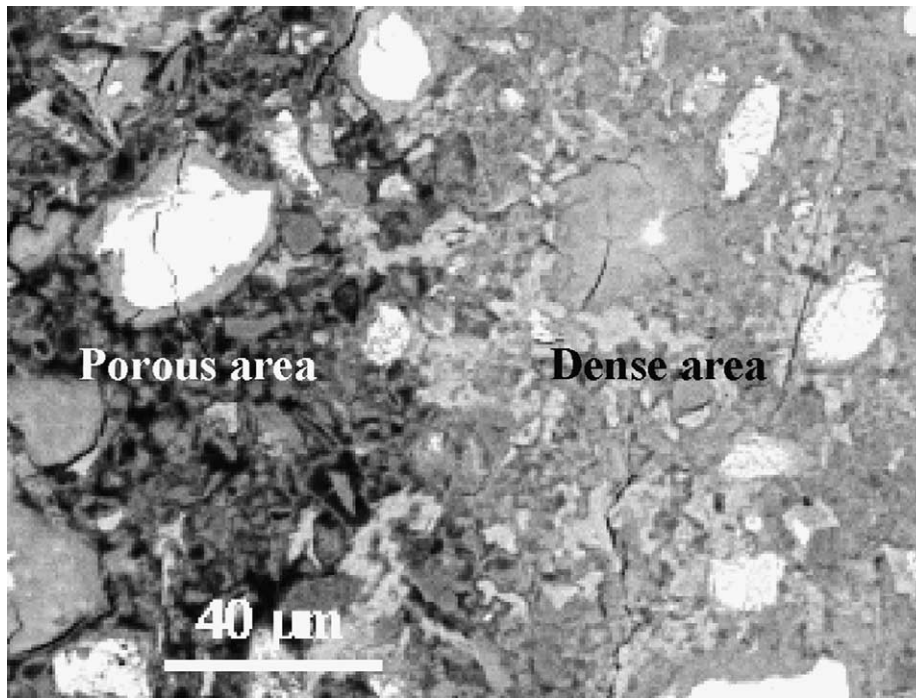


Fig. 13. Sharp boundary between adjacent patches of porous hcp (left) and dense hcp (right) in a laboratory mortar. Details were provided in [19].

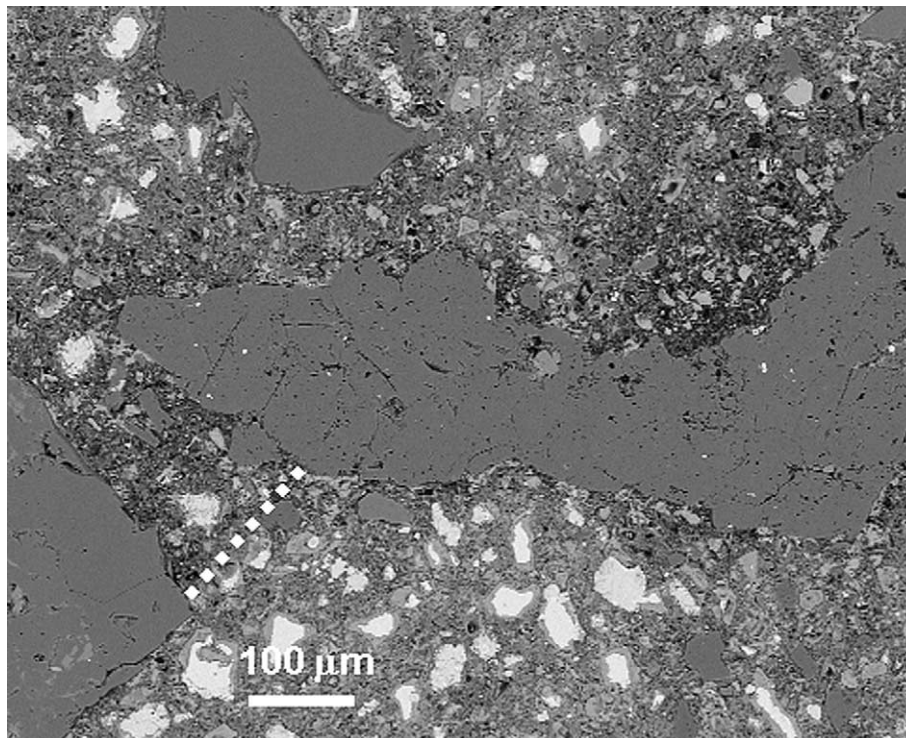


Fig. 14. Area showing dense and porous patches in a laboratory-mixed w:c 0.50 concrete hydrated for 28 days. A sharp boundary occurs at the dashed line; boundaries in other areas are more diffuse.

magnification. It is often possible to distinguish zones or patches of relatively dense paste containing little observable porosity which are distinct from zones or patches of obviously much higher local porosity. The porous zones tend to be irregular in shape and variable in size, but of the order of several hundred μm or more. Porous patches may partly encompass (or occasionally completely encompass) small sand grains, but they also spread through ‘bulk’ cement paste. In some places adjacent dense and porous patches show particularly sharp boundaries.

An exposition of such irregularly alternating porous/less porous patches of paste in a particular mortar was recently published by the present writer [19]. Fig. 13, reproduced from [19], shows an area with a sharp boundary between a porous area (on the left) and a dense area (on the right). The differences in local porosity are obvious.

That similar dense and porous patches occur in conventionally mixed concrete is indicated in Fig. 14, taken from a w:c 0.5 laboratory concrete mixed in a conventional pan mixer and hydrated for 28 days in a fog room at room temperature. A sharp boundary similar to that shown in Fig. 13, occurs at the dashed line. The porous area extends upward and around the long crushed dolomite aggregate grain, but the boundary in the upper part of the figure is more diffuse.

5. Discussion

The present paper represents a compilation of micrographs illustrating what the writer considers to be the important features of the internal architecture of cement paste as seen in backscatter-mode SEM. The micrographs themselves do not purport to represent the state-of-the-art in SEM photography; and indeed many of the figures used to illustrate the various structures were acquired some years ago. However, the writer hopes that the images selected and the accompanying discussion will help to promote a clearer and more definite picture of the internal structure of hcp and of hcp as it occurs in ordinary concrete.

Acknowledgements

The writer is grateful to his colleagues and former graduate students who have shared and furthered his interest in cement microstructure over a period of many years.

References

- [1] Scrivener KL. Backscattered electron imaging of cementitious microstructures: understanding and quantification. *Cem Concr Compos*, this issue [doi:10.1016/j.cemconcomp.2004.02.029].
- [2] Krinsley DH, Pye K, Boggs Jr S, Tovey NK. Backscattered scanning electron microscopy and image analysis of sediments and sedimentary rocks. Cambridge: Cambridge University Press; 1998.
- [3] Kjellsen K, Justnes H. Revisiting the microstructure of hydrated tricalcium silicate—a comparison to Portland cement. *Cem Concr Compos*, this issue [doi:10.1016/j.cemconcomp.2004.02.030].
- [4] Stutzman P, Clifton R. Specimen preparation for scanning electron microscopy. In: Jany L, Nispersos A, editors. *Proceedings 21st Int Conf on Cement Microscopy*, Las Vegas. Duncanville, TX: ICMA; 1999. p. 10–22.
- [5] Kjellsen KO, Monsøy A, Isachsen K, Detwiler RJ. Preparation of flat-polished specimens for SEM-backscattered electron imaging and X-ray microanalysis—importance of epoxy impregnation. *Cem Concr Res* 2003;33(4):611–6.
- [6] Diamond S. Digital image publication for backscatter SEM micrographs. *Cem Concr Res* 1996;26(1):3–7.
- [7] Scrivener KL, Pratt P. Backscattered electron images of polished cement sections in the scanning electron microscope. In: Bayless J, editor. *Proceedings 6th Int Conf on Cement Microscopy*, Albuquerque. Duncanville, TX: ICMA; 1984. p. 145–55.
- [8] Stutzman P. Scanning electron microscopy imaging of hydraulic cement. *Cem Concr Compos*, this issue [doi:10.1016/j.cemconcomp.2004.02.043].
- [9] Taylor HFW. *Cement chemistry*. 2nd ed. London: Thomas Telford; 1997.
- [10] Diamond S, Bonen D. A re-evaluation of hardened cement paste microstructure based on backscatter SEM investigations. In: Diamond S, Mindess S, Glasser FP, Roberts LW, Skalny JP, Wakeley LD, editors. *Microstructure of Cement-Based Systems/Bonding and Interfaces in Cementitious Materials*, Materials Research Society Symposium Proceedings, vol 370. Pittsburgh: Materials Research Society; 1995. p. 13–22.
- [11] Zhang Z, Olek J, Hill R. Microstructure of mortars at different stages of hydration. In: *Proceedings 25th Int Conf on Cement Microscopy*, Richmond. Duncanville, TX: ICMA; 2003 (publication in CD-Rom format).
- [12] Hadley D. The nature of the paste–aggregate interface. PhD thesis. Purdue University, West Lafayette, IN, 1972.
- [13] Hadley D, Dolch WL, Diamond S. On the occurrence of hollow-shell hydration grains in hydrated cement paste. *Cem Concr Res* 2000;30(1):1–6.
- [14] Diamond S. Calcium hydroxide in cement paste and concrete—a microstructural appraisal. In: Skalny JP, editor. *Materials Science of Concrete, Special Volume: Calcium Hydroxide in Concrete*. Westerfield, OH: American Ceramic Society; 2001. p. 37–58.
- [15] Sahu S, Badger S, Thaulow N, Lee, RJ. Determination of water:cement ratio of hardened concrete by scanning electron microscopy. *Cem Concr Compos*, this issue [doi:10.1016/j.cemconcomp.2004.02.032].
- [16] Diamond S. Mercury porosimetry: an inappropriate method for the measurement of pore size distributions in cement-based materials. *Cem Concr Res* 2000;30(10):1517–25.
- [17] Scrivener KL. The microstructure of concrete. In: Skalny J, editor. *Materials Science of Concrete*, vol 1. Westerfield, OH: American Ceramic Society; 1989. p. 127–62.
- [18] Bache HH, Idorn GM, Nepper-Christiansen P, Nielsen J. Morphology of calcium hydroxide in cement paste. In: *Special Report 90, Symposium on Structure of Portland Cement Paste and Concrete*, Highway Research Board, Washington, 1966. p. 154–74.
- [19] Diamond S. Percolation due to overlapping ITZs in laboratory mortars? A microstructural evaluation. *Cem Concr Res* 2003;33(7):949–55.